EUROPEAN ORGANIZATION FOR NUCLEAR RESEARCH

HIE-ISOLDE-PROJECT-Note-0003

HIE-LINAC and Beam lines for HIE-ISOLDE experiments

M. Pasini

Abstract

The document gives a brief description of the upgrade of the present REX-ISOLDE linac with a proposal for two possible solutions for the beam lines at high energy.

HIE-ISOLDE-PROJECT-Note-0003
3 Nov 2008

Geneva, Switzerland

November 2008

1 INTRODUCTION

In the present REX-ISOLDE facility [1] the Radioactive Ion Beams (RIBs) are accelerated to high energies with a compact Normal Conducting (NC) linac, making use of a special low energy preparatory scheme where the ion charge state is boosted so that the maximum mass to charge ratio is always $3 < A/q < 4.5$. This scheme consists of a Penning trap (REXTRAP), a charge breeder (REXEBIS) and an achromatic A/q separator of the Nier spectrometer type. The NC accelerator is designed with an accelerating voltage for a corresponding maximum A/q of 4.5 and it delivers a final energy of 3 MeV/u for $A/q < 3.5$ and 2.8 for $A/q < 4.5$. After charge breeding, the first acceleration stage is provided by a 101.28 MHz 4-rod Radio Frequency Quadrupole (RFQ) which takes the beam from an energy of 5 keV/u up to 300 keV/u. The beam is then re-bunched into the first 101.28MHz interdigital drift tube (IH) structure which increases the energy to 1.2 MeV/u. Three split ring cavities are used to give further acceleration to 2.2 MeV/u and finally a 202.58 MHz 9-gap IH cavity is used to boost and to vary the energy between $2 < E < 3$ MeV/u. Fig. 1 illustrate the scheme of the present linac.

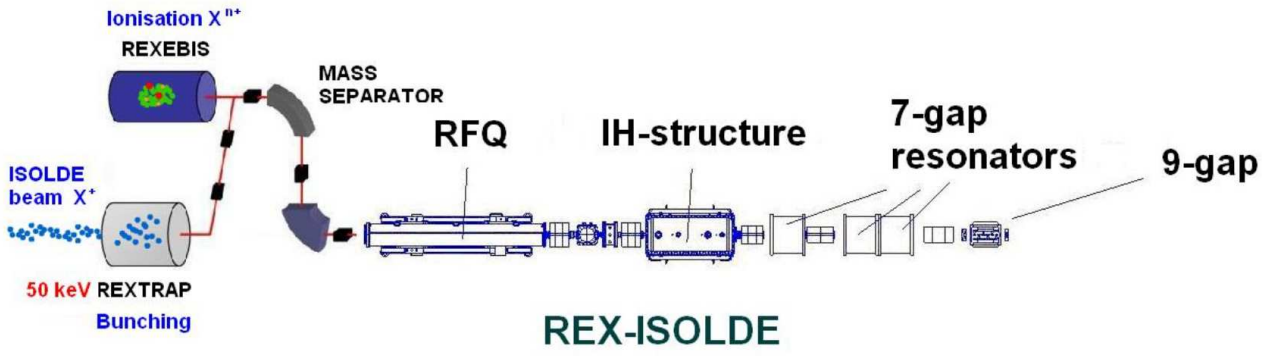

Figure 1: REX-ISOLDE present scheme.

The HIE-ISOLDE project contains three major parts: higher energies, improvements in beam quality and flexibility, and higher beam intensities. This requires developments in radioisotope selection, improvement in charge breeding and target-ion source development, as well as construction of the new injector for the PSB, LINAC4. The most significant improvement in the physics program [2] will come from the energy upgrade which aims at reaching a minimum energy of 10 MeV/u.

The present NC machine was developed in order to deliver beams at specific energies whilst taking advantage of the high accelerating gradient that pulsed NC IH structure could achieve. This concept is nevertheless not without some limitations: 1) limited energy variability; 2) operation restricted to pulsed mode; 3) inefficient use of the installed power when running light ions; 4) non variable longitudinal beam parameters, such as energy spread and bunch length.

To overcome the above limitations a superconducting linac based on Nb-sputtered SC Quarter Wave Resonators (QWRs) has been proposed [3].

2 THE SUPERCONDUCTING LINAC

The superconducting linac is designed to deliver an effective accelerating voltage of at least 39.6 MV with an average synchronous phase ϕ_s of -20 deg. This is the minimum voltage required in order to achieve a final energy of at least 10 MeV/u with $A/q = 4.5$. Because of the steep variation of the ions velocity, at least two cavity geometries are required in order to have an efficient acceleration throughout the whole energy range. A total number of 32 cavities are needed to provide the full acceleration voltage. The geometries chosen corresponding to *low* ($\beta_0 = 6.3\%$) and *high* ($\beta_0 = 10.3\%$) "β" cavities maintain the fundamental beam frequency of 101.28 MHz and their design parameters are given in Table 1. The

design accelerating gradient aims at reaching 6 MV/m with a power consumption of 7 W per low β cavity and 10 W per high β cavity.

Table 1: Cavity design parameters

Cavity	**Low** β	**high**β
No. of Cells	2	2
f (MHz)	101.28	101.28
β_0 (%)	6.3	10.3
Design gradient E_{acc}(MV/m)	6	6
Active length (mm)	195	300
Inner conductor diameter (mm)	50	90
Mechanical length (mm)	215	320
Gap length (mm)	50	85
Beam aperture diameter (mm)	20	20
$U/{E_{\text{acc}}}^2$ (mJ/(MV/m)^2	73	207
$E_{\text{pk}}/E_{\text{acc}}$	5.4	5.6
$H_{\text{pk}}/E_{\text{acc}}$ (Oe/MV/m)	80	100.7
R_{sh}/Q (Ω)	564	548
$\Gamma = R_{\text{s}} \cdot Q_0$ (Ω)	23	30.6
Q_0 for 6MV/m at 7W	$3.2 \cdot 10^8$	$5 \cdot 10^8$
TTF max	0.85	0.9
No. of cavities	12	20

Because each cavity is independently phased, we can apply the maximum voltage available in each cavity so that lighter ion will reach higher final energies. Figure 2 shows a plot of the energies reached by the ions with different A/q.

The installation of the superconducting linac is foreseen in two main stages; the first one consists of installing 10 high β cavities grouped in two cryomodules downstream of the present NC linac (stage 1). The second stage will be installed in two parts. Firstly, two more high β cryomodules will be added (stage 2a) downstream from those in stage 1 and secondly the split ring cavities and the 202.56 MHz IH cavity will be replaced with 12 low β cavities grouped in 2 cryomodules (stage 2b). Figure 3 shows a schematic of the different installation stages. The final energy for stage 1 and stage 2 is respectively 5.5 MeV/u and 10 MeV/u for A/q=4.5.

The focusing scheme foresees the employment of 200 mm long SC solenoids, which allow a high mismatch factor tolerance with respect to a standard triplet or doublet focusing scheme [4]. This brings a significant advantage for the tuning and operation of the machine. In fact, RIBs accelerators in general make use of a *high* intensity stable beam as a pilot beam with an A/q ratio that is as close as possible to the A/q of the wanted RIB. This is in fact necessary, since the very low RIB's intensity is practically invisible to conventional beam instrumentation. Once the pilot beam is established, a scaling action is performed and a focusing lattice with high mismatch tolerance guarantees better beam transport in the machine after scaling, where possible beam mismatch can occur. A schematic of the two cryomodules is shown in Figure 4. With this configuration the beam diagnostics instruments are ideally positioned at the beam waist location in the inter-cryomodule region where a pair of steering magnets will also be installed.

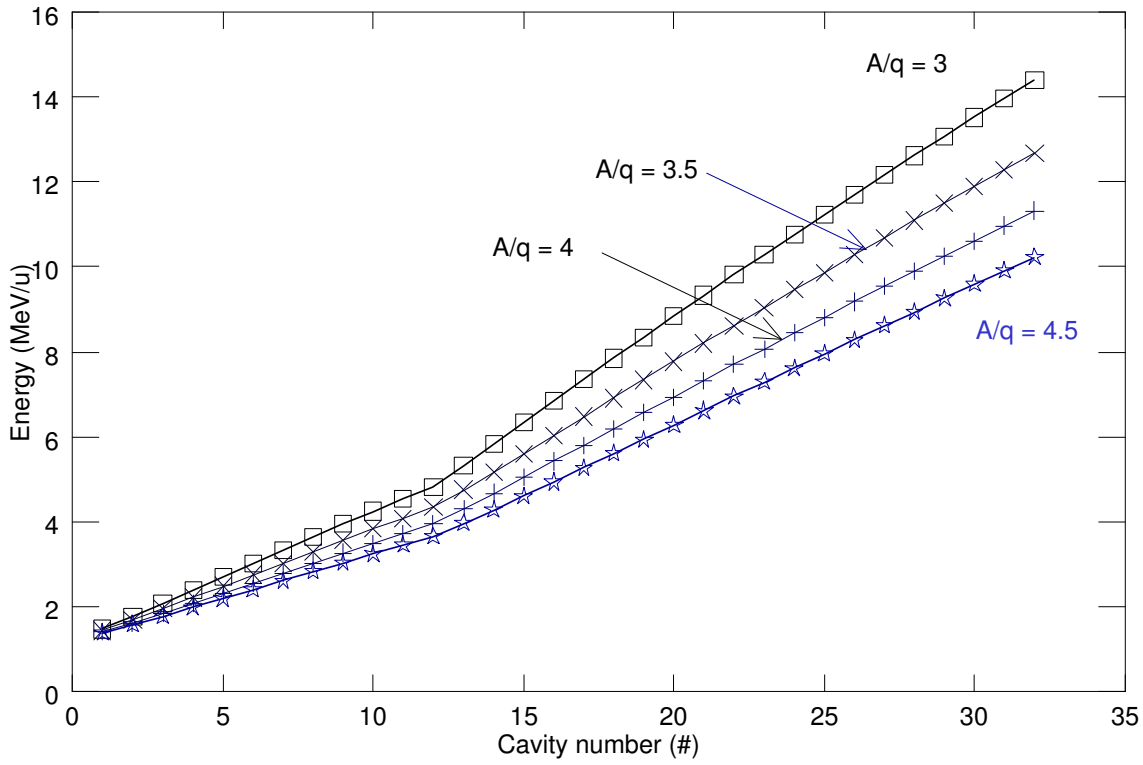

Figure 2: Beam energy as a function of the cavity number. For the $A/q = 3$ the maximum energy achieved is 14.4 MeV/u

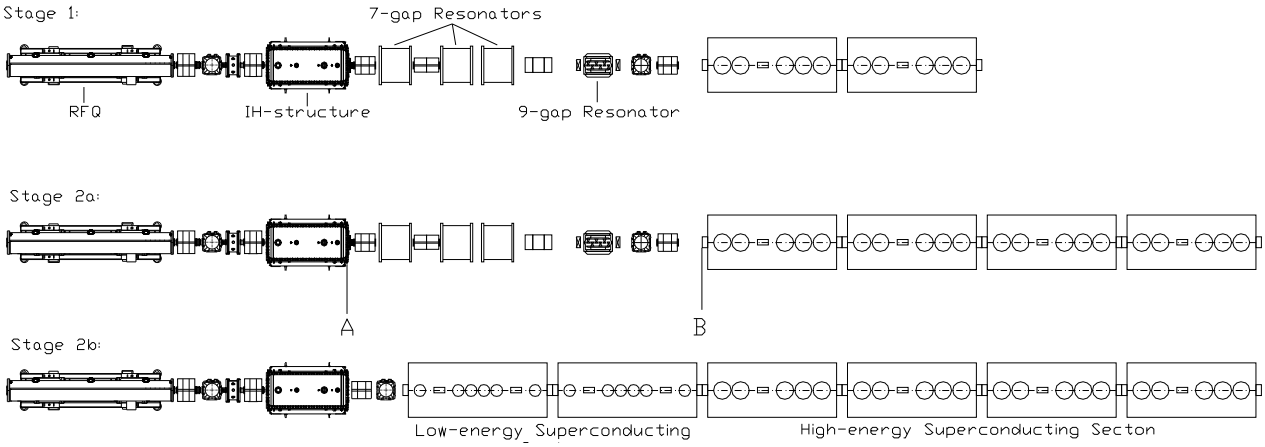

Figure 3: A Schematic of the HIE-ISOLDE linac stages. Stage 1 is shown at the top, while stage 2 can be split into two sub-stages depending on the physics priorities: the low energy cryomodules will allow the delivery of a beam with better emittance; the high energy cryomodule will enable the maximum energy to be reached

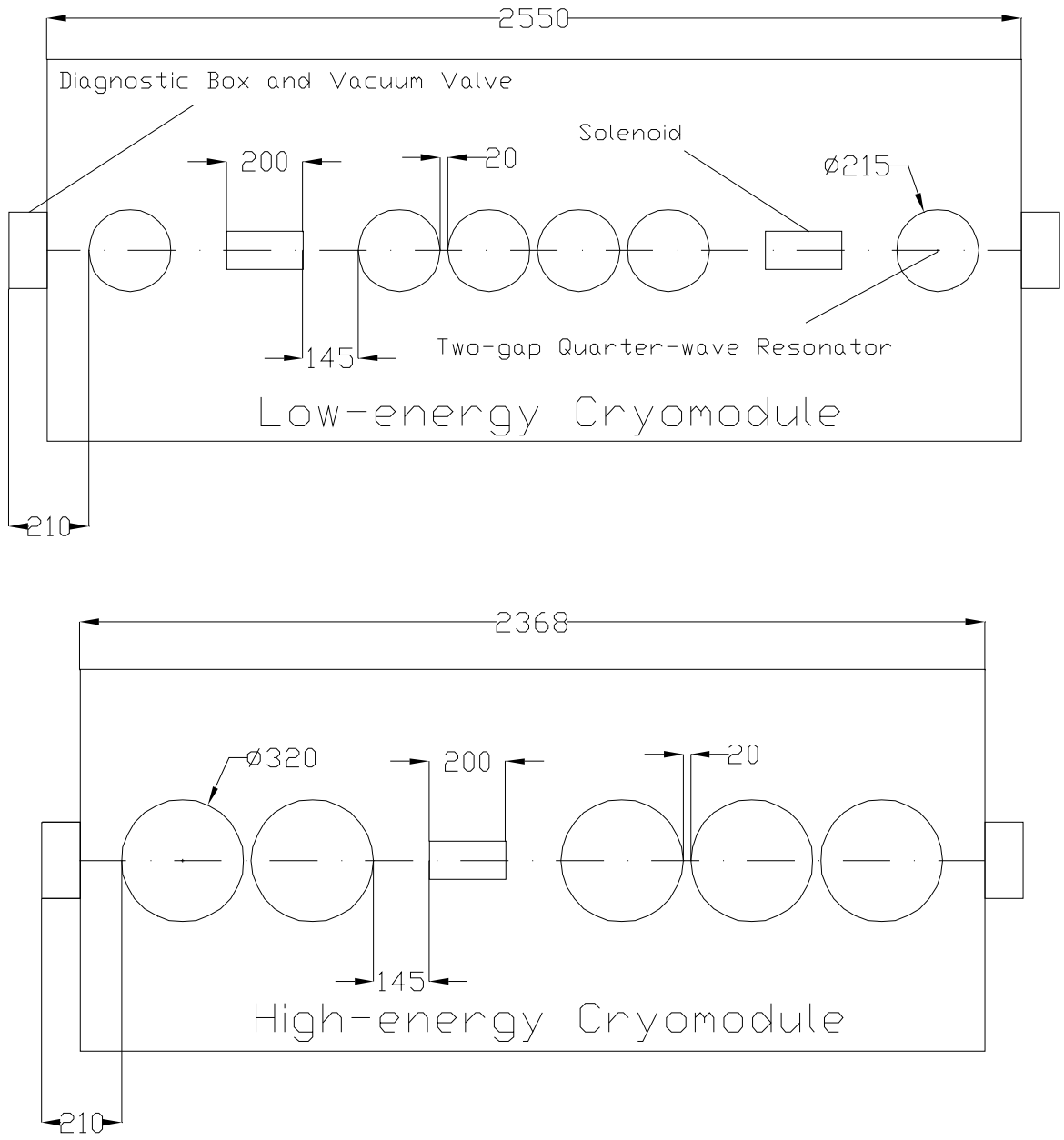

Figure 4: Schematic of the cryomodules design. On the top the low β cryomodule and on the bottom the high β cryomodule. In the figure a value of 210mm has been taken as a length of half of the intermodule distance. This value value is important for the definition of the overall linac length and it depends on the choice of the cryomodule technology, i.e. separate or common vacuum (see section later).

3 BEAM DYNAMICS SIMULATIONS

For the simulations of the complete HIE-LINAC (stage 2b) a 1 m long matching section with 4 quadrupoles between the first IH-structure and the first cryomodule is taken into account. It is important to keep this section as short as possible in order to minimize the longitudinal beam debunching. The input beam parameters for the simulations are constrained by the IH-cavity output beam and were calculated using `TRACE3D` [5]. The resonators were set to operate at a synchronous phase of -20 deg., and to increase the longitudinal phase spread capture at injection, the first resonator was phased at -40 deg. The last resonator in the first cryomodule was also re-phased, at -30 deg., in order to further decrease the longitudinal phase spread of the beam after the first cryomodule. The simulations were implemented to first-order in `LANA` [6] using a square field distribution for the cavities and solenoids and the results confirmed with `Path Manager` [7], which uses a thin-lens approximation for lattice elements. Two thousand particles were simulated and space-charge forces neglected because of the low beam intensity.

The solenoidal magnetic fields were adjusted to achieve matched beams along the HIE-LINAC. The three solenoids in the second and third cryomodules were used to match the beam across the transition region between the low and high-energy sections. Matched solutions were found for different values of the phase advance per cryomodule μ in the low-energy section and the resulting transverse emittance growth along the HIE-LINAC investigated. We report here our reference solution, which corresponds to a phase advance per solenoidal period $\mu = 90$ deg. (Fig. 5)

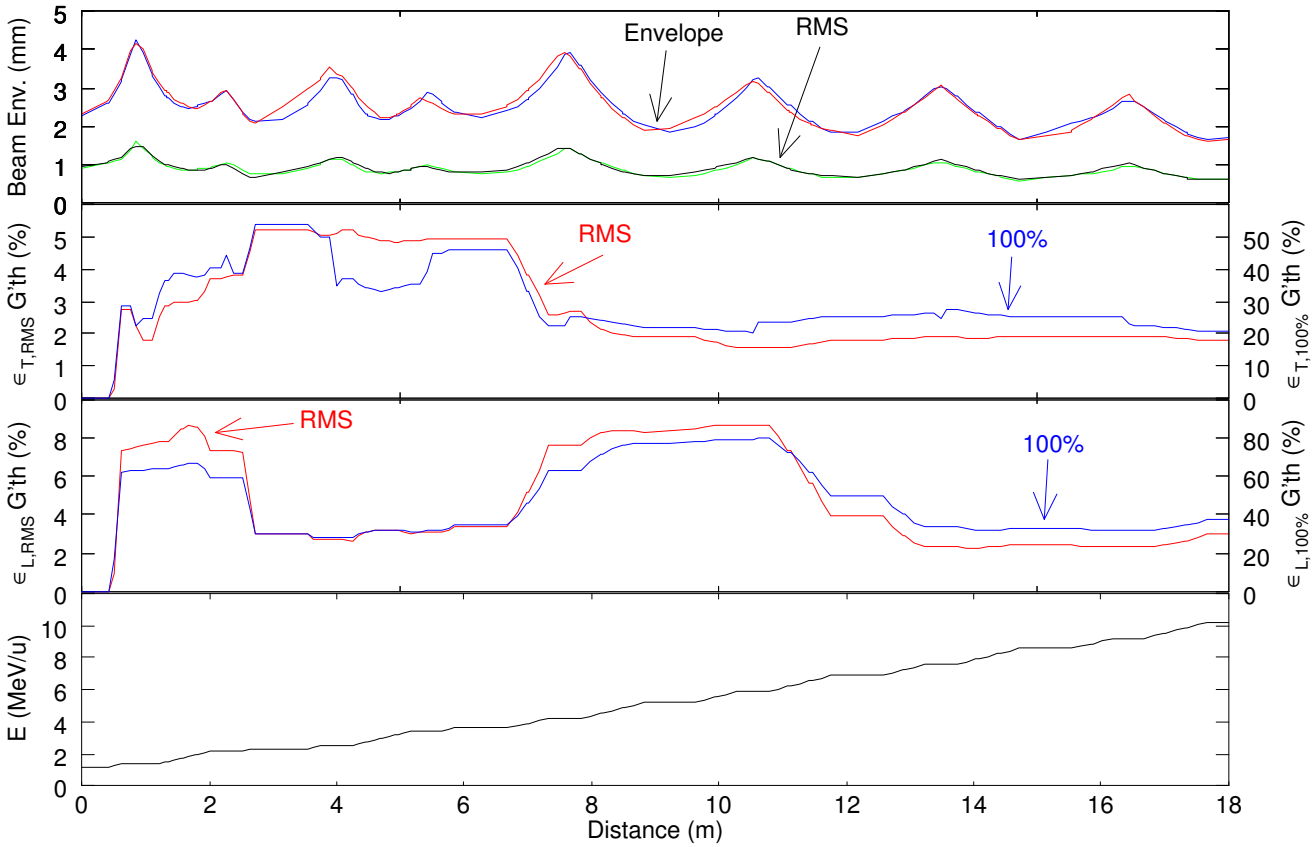

Figure 5: Beam dynamic for a simulation with phase advance of 130 and 90 deg. in the low and high-energy sections, respectively. From top to bottom: max and rms envelope, 100% and rms transverse emittance growth, 100% and rms longitudinal emittance growth, beam energy as a function of the linac length

The input and output beam parameters are listed in Table 2 for the two installation stages. The

average solenoidal magnetic field in the low-energy section is 5.1 T and 7.4 T in the high-energy section.

Table 2: Beam Parameters

Parameter	**Input**	**Output**
Stage 1		
α_T	-0.150	-0.165
β_T (cm/mrad)	0.100	0.132
$\epsilon_{T,100\%,\text{norm}}$ (π cm mrad)	0.030	0.037
α_L	1.425	-0.355
β_L (deg/keV)	0.027	0.038
$\epsilon_{L,100\%,\text{norm}}$ (π ns keV/u)	2.000	2.517
Stage 2		
α_T	-0.200	-0.209
β_T (cm/mrad)	0.100	0.138
$\epsilon_{T,100\%,\text{norm}}$ (π cm mrad)	0.030	0.036
α_L	1.281	1.013
β_L (deg/keV)	0.035	0.044
$\epsilon_{L,100\%,\text{norm}}$ (π ns keV/u)	2.000	2.746

4 CRYOMODULES

The choice of having a SC solenoid as focusing element allows to reduce the intermodule distance with respect to a scheme where the focusing elements are made of warm quadrupoles. The advantage is a more compact linac, saving precious space for the experiments and simplify the longitudinal beam dynamics. An important design issue of low energy SC ion linacs is whether the beam vacuum is shared with the insulation vacuum or not. Figure 6 illustrates the two concepts of cryomodules with single or separate vacuum. In the former, the cavities and solenoid beam tubes are open to the cryostat envelope, and no long interconnection region are necessary as there is no direct thermal conductivity through a beam pipe. The separate vacuum concept features an additional vessel, creating a second vacuum envelope around the the cavities and solenoids, the putting a direct metal thermal contact between the 4K and the 300K region. This solution carries a longer intercryomodule distance with a consequent longer linac (it is estimated at least 2.5 m more).

5 CRYOPLANT

The cryoplant needed to supply liquid helium at 4.5 K will require an additional building - located next to the experimental hall - to house the compressor station and its cold box. We are looking at the possibility of reusing an existing refrigerator which was connected to the ALEPH magnet during the LEP operation from 1989 to 2000. The cold box was capable in 1989 to provide an isothermal refrigeration power of 630W at 4.5K plus an additional shield load of 2700 W between 55K and 75K. Fig. 7 shows a first concept design of the cryoplant. The total heat load of the system required for the complete ISOLDE energy upgrade is very close to the maximum power that the cold box can provide. Nevertheless, we have to evaluate precisely this possibility as it would allow a substantial cost saving with respect to the purchase of a new unit. The transfer line needed to supply the liquid helium is 35 m long and will be equipped with 6 *jumper* modules (one per module) to allow the isolation of each module from the common distribution line without interruption on the remaining modules.

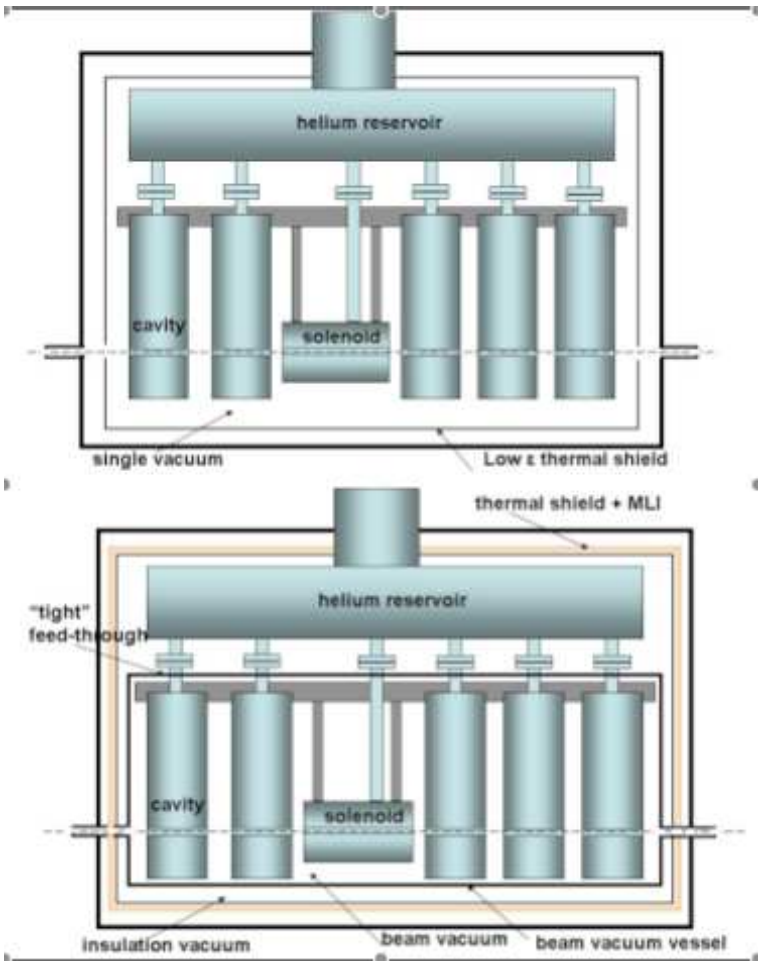

Figure 6: Single vacuum (top) and separate vacuum(bottom) concepts.

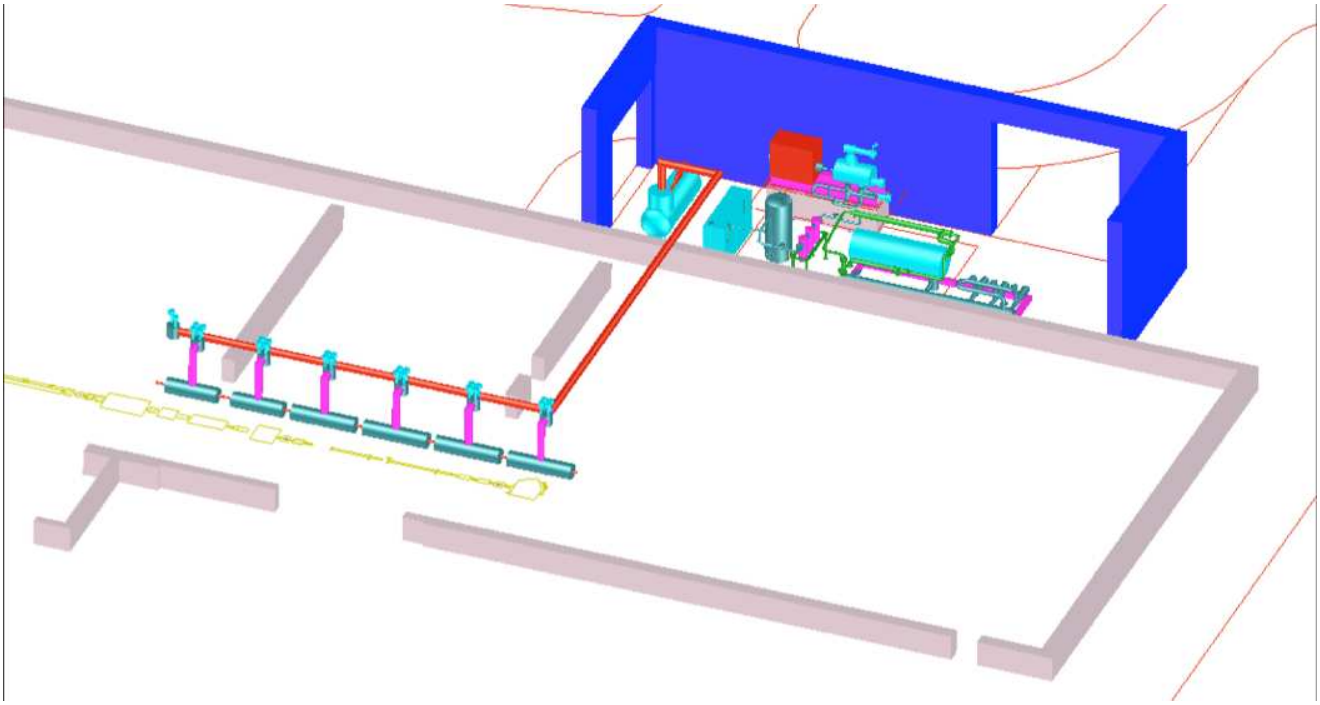

Figure 7: Cryoplant 3-D layout

6 High Energy Beam Transport - HEBT

For the beam transport to the experimental station we propose here two solutions based on the following assumptions:

1. The linac length is 16.86m; this length consider a intercryomodule distance of 600 mm and the cryomodule share the beam vacuum with the insulation vacuum.
2. The matching section between the IH cavity and the SC linac is 1 m long
3. The end of the linac is 5.075m inside the new experimental hall

Fig. 8 shows the first solution proposed

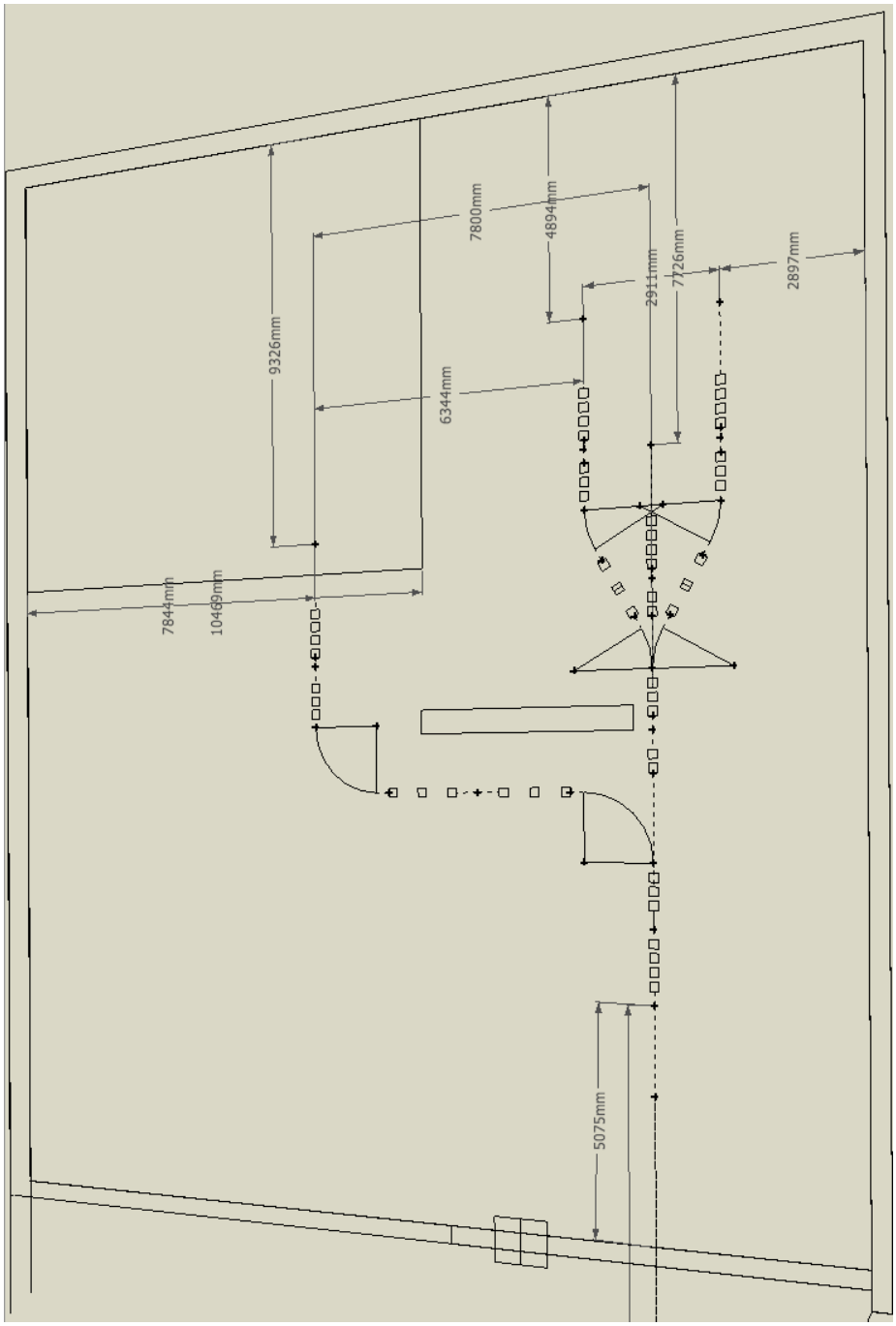

Figure 8: option1

In this solution we propose to have a focus point after the linac from which we can either bend the beam to a 90 deg achromatic chicane where the height can be adjusted or after a short straight section the beam can go to one of the two 30deg chicanes. In the first line the remaining space is asquare of roughly 10 by 10 m^2, while in the seconds lines the distance from the target position to the wall is roughly 4.8 m. This solution allows also to have a measurement line in the straight line that could be used in parallel as beam quality measurement line.

Fig. 9 shows the second solution proposed Differently from the previous solution, in this case the

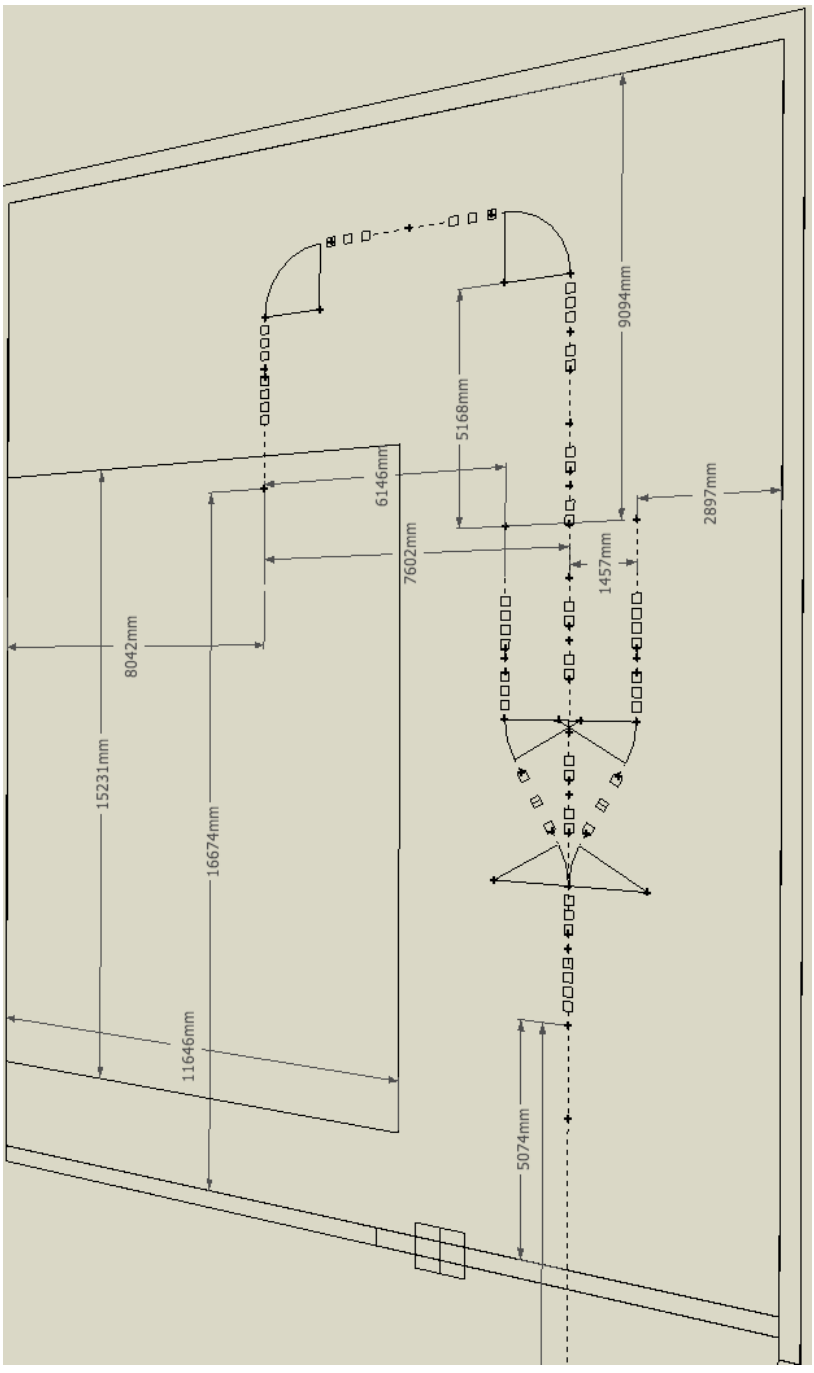

Figure 9: option2

beam is either sent to a 30 deg chicane or to a 180 deg achromatic bending section which is positioned at the far end of the extension hall. This configuration allows to gain a significant space which can be used for the installation of a several experimental instruments; the new area available is in fact 11 by 15 m^2.

The HEBT line consists of several modular section, each of them solving a particular function of the beam transport:

- linac matching section: 4 quadrupole are used to match the beam coming out of the linac into the following section (Fig. 10)
- achromat bending section: we have defined 3 types of bending sections, one is a 180 deg achromat, one is dogleg typo of bending with 90 deg bending magnet and the last one is also a dogleg acrhomat but with 30 deg bending angle magnets. (Fig. 11 and 12 and 13)
- point to point doublet transport: 4 quads are used to linearly transport the beam from one focus point to another. (Fig. 14)
- final focus section: this section allow to focus the beam in the target in different beam sizes and convergence angle. (Fig. 15)

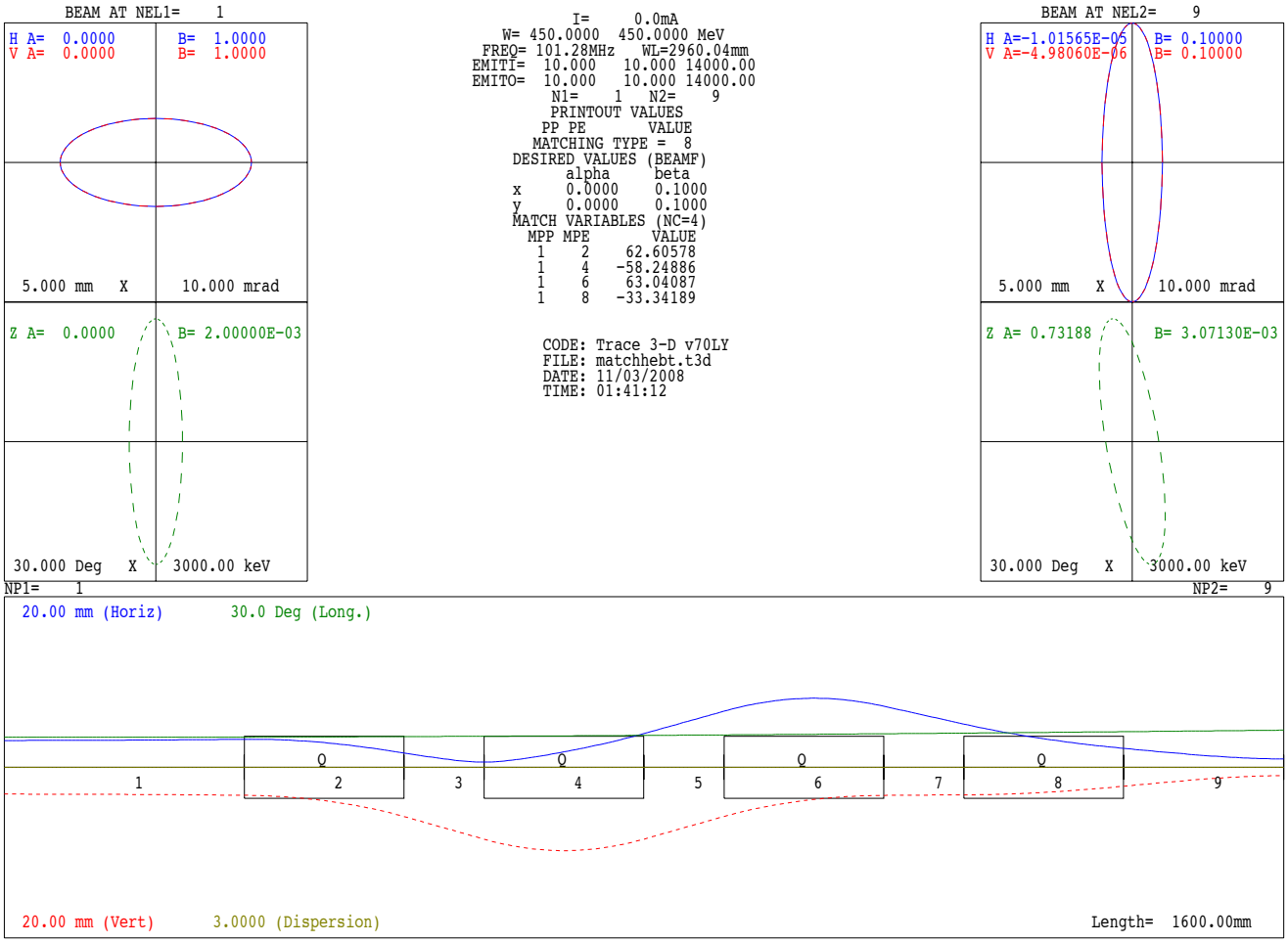

Figure 10: Matching section between the linac and the HEBT.

The two solution proposed are to be considered at ta very early design stage and don't take into consideration several aspect, such as physical size of the magnets and their integration. Requirements for the shielding is also not considered, but the modularity of the two option presented can accomodate any request in terms of distance between one beam line in the other. For the 90 deg chicane and 180 deg bending section we have considered the HMI dipoles for which the use at 10 MeV/u with A/q=4.5 is not guaranteed. (Stability test at high field need to be performed) The length of the linac is not frozen, so the final position and consequently the avaialble space of the experimental instruments can change. (It is estimated the error to be in the range of 1m)

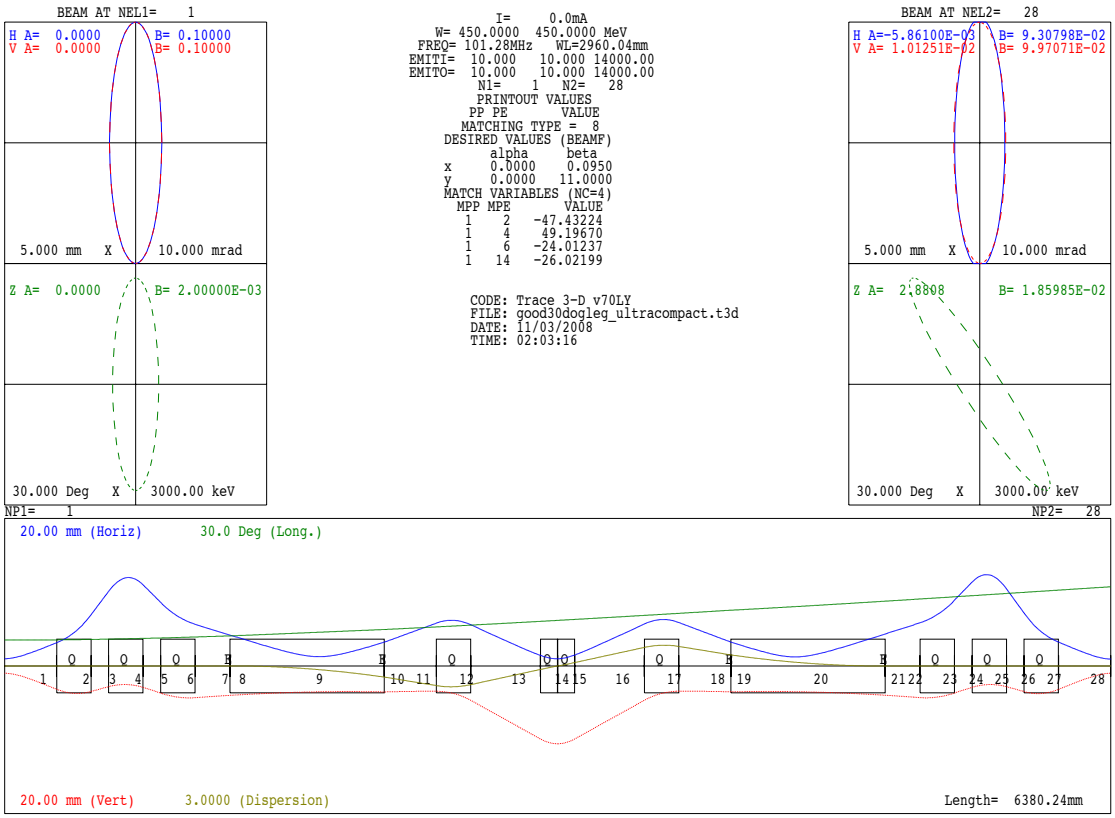

Figure 11: 30 deg chicane section; this part has been designed in order to minimise the longitudinal space requirements

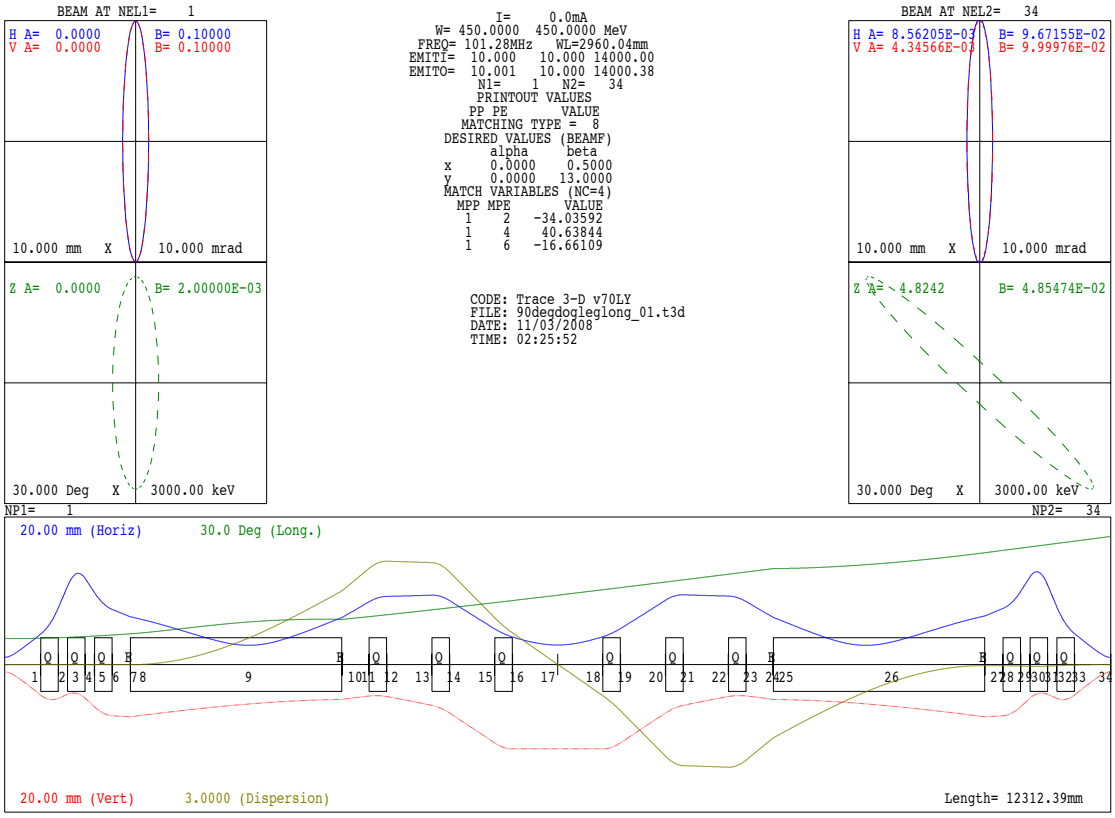

Figure 12: 90 deg chicane section; this part is design to be completely achromatic in position and angle. The distance between the two main dipoles is easily adjustable so to fit any space requirements

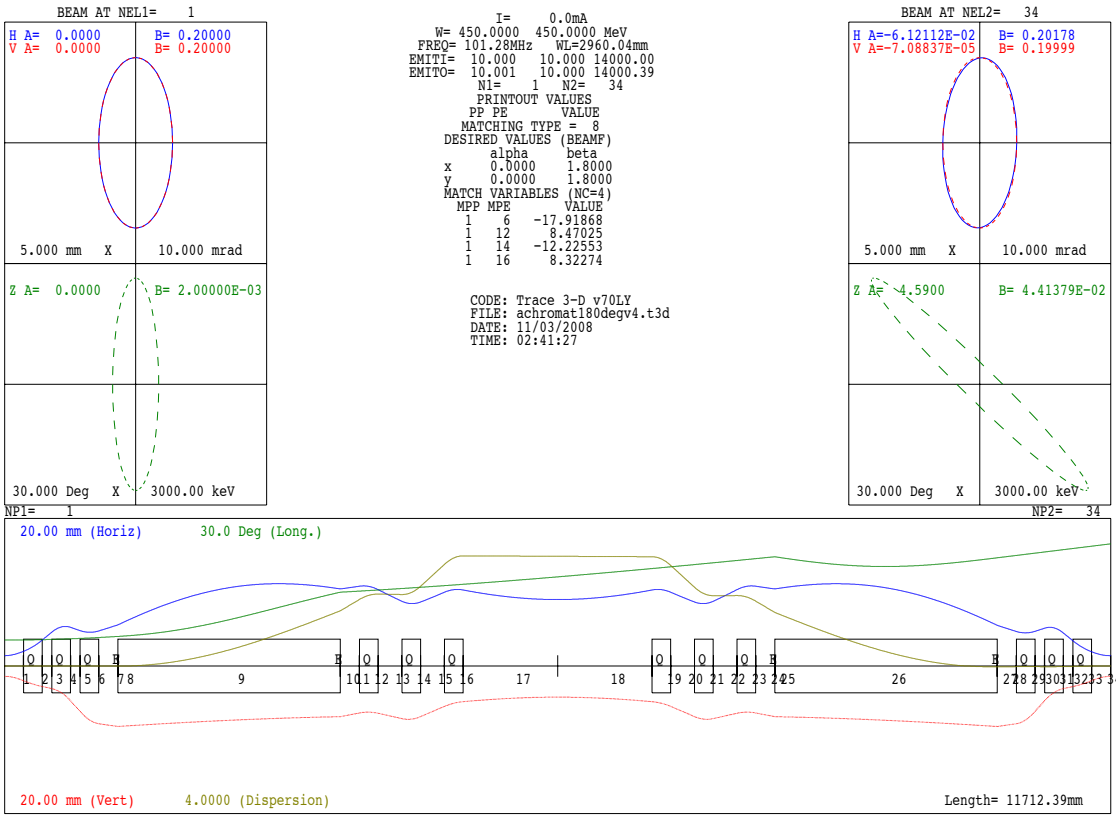

Figure 13: 180 deg bending section; this part has been designed to have a flexible distance between the two main dipoles.

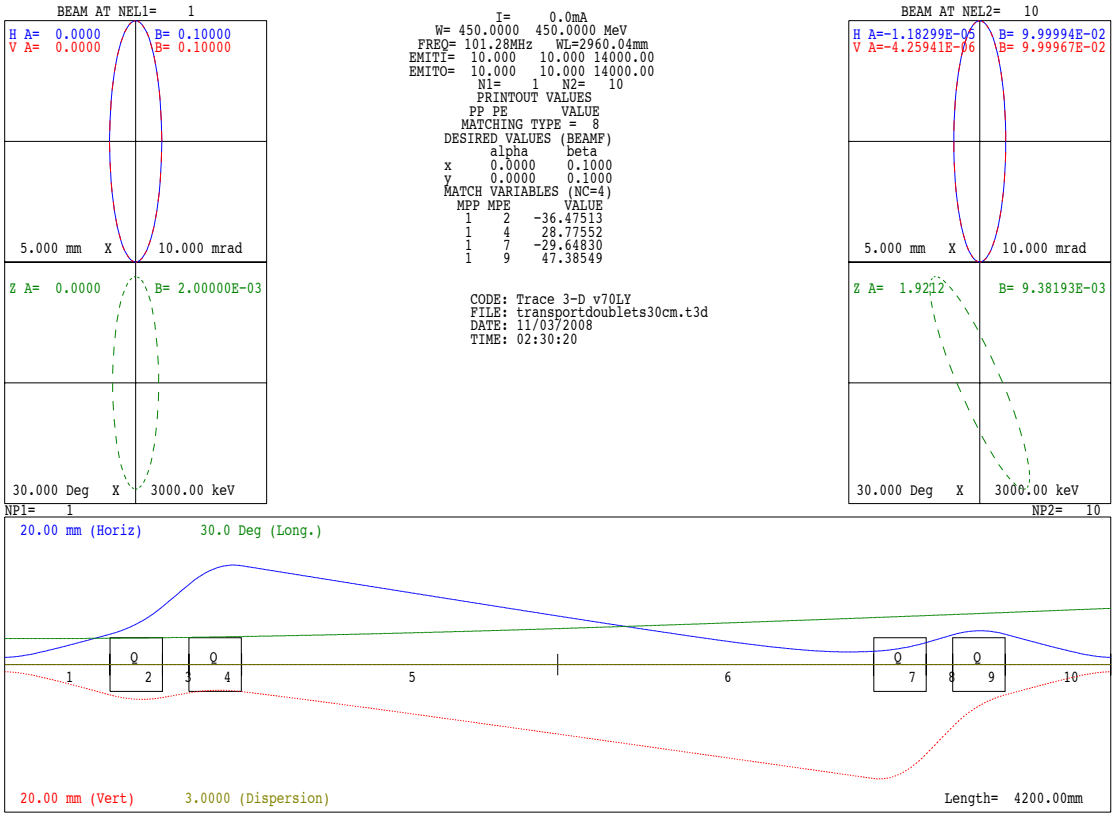

Figure 14: Linear transport section; this part has been designed so to have a flexible distance between the two focus point.

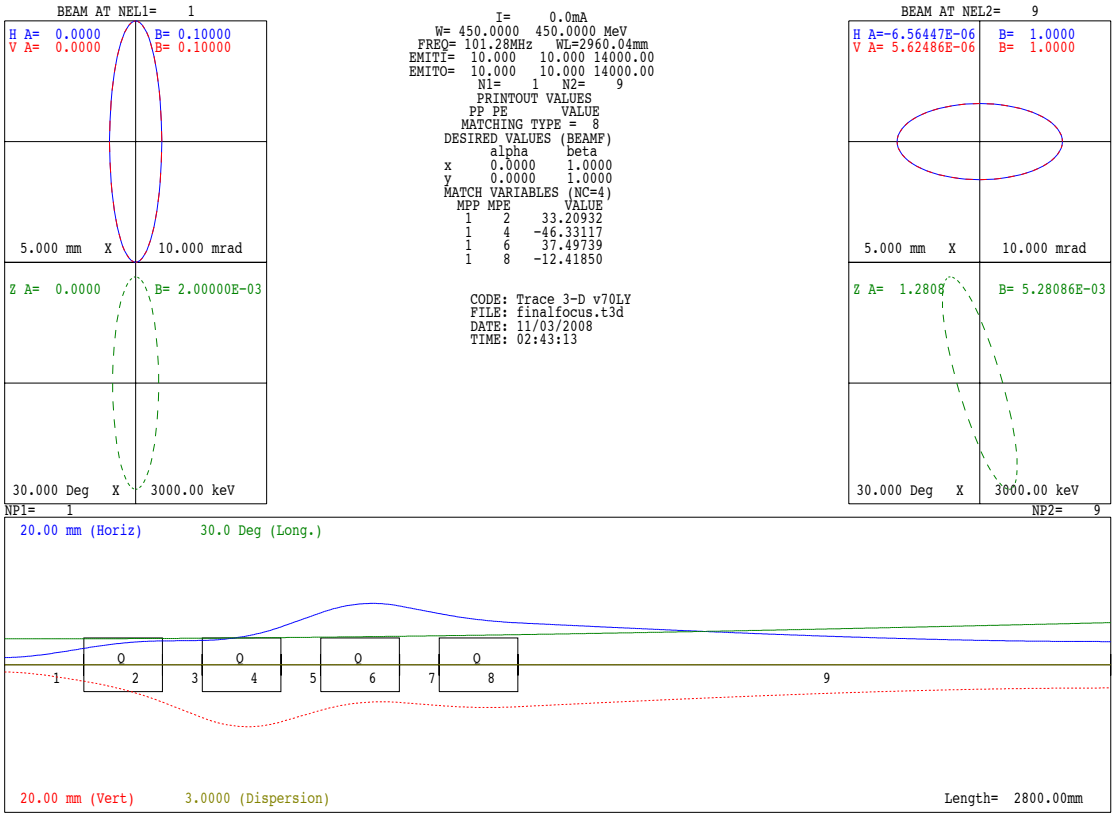

Figure 15: Target section; this part allows to produce several type of beam focus and convergence into an experimental target.

References

[1] D. Voulot, *et al*., Radioactive beams at REX-ISOLDE: Present status ..., Nucl. Instr. and Meth. B (2008), doi:10.1016/j.nimb.2008.05.129

[2] K. Riisager, *et al*. HIE-ISOLDE: the scientific opportunities, CERN-2007-008

[3] `http://hie-isolde.web.cern.ch`

[4] R. Laxdal, Initial Commissioning Results from the ISAC-II SC Linac, LINAC06, Knoxville, US

[5] K.R. Crandall *et al*., Trace 3-D Documentation, LA-UR-97-886

[6] D. V. Gorelov, P. N. Ostrumov, Application of LANA Code for Design of Ion Linac, Proc. of Linac Conference 1996

[7] A. Perrin and J.F. Amand, Travel v4.06, user manual, CERN (2003).